Neurotoxicology 70 (2019) 135–145

Contents lists available at ScienceDirect

Neurotoxicology

journal homepage: www.elsevier.com/locate/neuro

Soluble epoxide hydrolase inhibitor, APAU, protects dopaminergic neurons against rotenone induced neurotoxicity: Implications for Parkinson's disease

Navya Lakkappa[a], Praveen T. Krishnamurthy[a,*], Pandareesh M.D.[b], Bruce D. Hammock[c], Sung Hee Hwang[c]

[a] Department of Pharmacology, JSS College of Pharmacy, Ooty, India
[b] Department of Neurochemistry, National Institute of Mental Health & Neuro Sciences, Bangalore, India
[c] Department of Entomology and Nematology, and Comprehensive Cancer Research Center, University of California, Davis, United States

ARTICLE INFO

Keywords:
Parkinson
Soluble epoxide hydrolase
Epoxyeicosatrienoic acids
Neuroprotection
Oxidative stress
Inflammation
Apoptosis
APAU

ABSTRACT

Epoxyeicosatrienoic acids (EETs), metabolites of arachidonic acid, play a crucial role in cytoprotection by attenuating oxidative stress, inflammation and apoptosis. EETs are rapidly metabolised *in vivo* by the soluble epoxide hydrolase (sEH). Increasing the half life of EETs by inhibiting the sEH enzyme is a novel strategy for neuroprotection. In the present study, sEH inhibitors APAU was screened *in silico* and further evaluated for their antiparkinson activity against rotenone (ROT) induced neurodegeneration in N27 dopaminergic cell line and *Drosophila melanogaster* model of Parkinson disease (PD). In the *in vitro* study cell viability (MTT and LDH release assay), oxidative stress parameters (total intracellular ROS, hydroperoxides, protein oxidation, lipid peroxidation, superoxide dismutase, catalase, glutathione peroxidise, glutathione reductase, glutathione, total antioxidant status, mitochondrial complex-1activity and mitochondrial membrane potential), inflammatory markers (IL-6, COX-1 and COX-2), and apoptotic markers (JNK, phospho-JNK, c-jun, phospho-c-jun, pro and active caspase-3) were assessed to study the neuroprotective effects. *In vivo* activity of APAU was assessed in *Drosophila melanogaster* by measuring survival rate, negative geotaxis, oxidative stress parameters (total intracellular ROS, hydroperoxides, glutathione levels) were measured. Dopamine and its metabolites were estimated by LC-MS/MS analysis. In the *in silico* study the molecule, APAU showed good binding interaction at the active site of sEH (PDB: 1VJ5). In the *in vitro* study, APAU significantly attenuated ROT induced changes in oxidative, pro-inflammatory and apoptotic parameters. In the *in vivo* study, APAU significantly attenuates ROT induced changes in survival rate, negative geotaxis, oxidative stress, dopamine and its metabolites levels ($p < 0.05$). Our study, therefore, concludes that the molecule APAU, has significant neuroprotection benefits against rotenone induced Parkinsonism.

1. Introduction

Parkinson's disease (PD) is a second most common chronic progressive neurodegenerative disorder, characterised by selective loss of nigrostriatal dopaminergic neurons (Bonnet and Houeto, 1999; Cummings, 1992; De Virgilio et al., 2016; DeLong and Wichmann, 2009). One of the major pathological features of PD is the presence of Lewy bodies in neuronal cytoplasm, mainly composed of α-synuclein (α-syn) and ubiquitin (Spillantini et al., 1997; Stefanis, 2012). The current treatment strategies such as MAO inhibitors, COMT inhibitors,

Abbreviations: sEH, soluble epoxide hydrolase; EETs, epoxyeicosatrienoic acids; PD, Parkinson's disease; COX, cyclooxygenase; LOX, lipoxygenase; AA, arachidonic acid; MAO, monoamine oxidase; COMT, catechol-*O*-methyl transferase; APAU, 1-(1-acetypiperidin-4-yl)-3-adamantanylurea; ROT, rotenone; SOD, superoxide dismutase; ROS, reactive oxygen species; CAT, catalase; IL-6, Interleukin-6; EPHX-2, epoxide hydrolase 2; COX, cyclooxygenase; PDB, protein data bank; RMDS, root-mean-square deviation; GPx, glutathione peroxidase; GR, glutathion réductase; GSH, glutathione; ABTS, [22′-azinobis-(3-ethylbenzothiazoline-6-sulfonic acid)]; TAC, total antioxidant status; DNP, α-dinitrophenyl; HRP, horseradish peroxidase; JNK, c-jun N-terminal kinases; XP, extra precision; FBS, fetal bovine serum; RPMI, Roswell Park Memorial Institute; MTT, 3-(4,5-dimethylthiazol-2-yl)-2,5-diphenyltetrazolium bromide; LDH, lactate dehydrogenase; DCFDA, 2′,7′- dichlorfluorescein-diacetate; TBARS, thiobarbituric acid; MDA, malondialdehyde; MMP, mitochondrial membrane potential; DTNB, 5, 5′ dithiobis 2-nitrobenzoic acid; DNPH, 2,4-dinitrophenylhydrazine; HEPES, (4-(2-hydroxyethyl)-1-piperazineethanesulfonic acid); EGTA, Ethylene Glycol Bis(2-aminoethyl Ether)tetraacetic Acid; DMSO, dimethyl sulfoxide; DA, dopamine; DOPAC, 3,4-dihydroxyphenylacetic acid; HVA, homovanillic acid; IS, internal standard

* Corresponding author.
E-mail address: praveentk7812@gmail.com (P.T. Krishnamurthy).

https://doi.org/10.1016/j.neuro.2018.11.010
Received 7 August 2018; Received in revised form 12 November 2018; Accepted 13 November 2018
Available online 22 November 2018
0161-813X/

Levodopa, and surgery are focused on the motor and non-motor complications and therefore provide only symptomatic relief (Quinn, 1995; Schapira, 2005). Levodopa and other medications drastically improve the motor symptoms and quality of life of patients with PD in the early stages. Soon later, the patients suffer from dopa-resistant motor symptoms (impairment of speech, posture, and balance), DOPA-resistant nonmotor signs (impairment of mood, sleep and cognition) and drug-related side effects (psychosis, motor fluctuations, gait impairment and dyskinesias) such as hallucinations, dementia, depression, swallowing problem, sleep disorder, constipation, fatigue *etc.* Unfortunately, none of the anti-parkinsonian therapies, alone or in combination have the ability to halt disease progression on a long-term basis (Caraceni et al., 1989; Esposito and Cuzzocrea, 2010; Jankovic and Aguilar, 2008; Oertel and Schulz, 2016; Rascol et al., 2003b). It is, therefore, important to halt disease progression with neuroprotective agents to effectively manage this disease (Rascol et al., 2003b). The major pathological mechanisms contributing to neurodegeneration are oxidative stress and inflammation which in turn contribute to mitochondrial dysfunctioning, protein aggregation and apoptosis (Morisseau and Hammock, 2013a; Mullin and Schapira, 2015; Perfeito et al., 2012). Hence there is a need to develop molecules which can simultaneous attenuate oxidative stress, inflammation and resulting apoptosis in PD.

In the current study, the rotenone being one of the naturally occurring insecticide and herbicide was used to closely mimic pathophysiology of the PD. Rotenone is a highly lipophilic compound and readily crosses the blood–brain barrier. It is reported to inhibit complex-1 activity and causes destruction of dopaminergic neurons through oxidative and inflammatory reactions (Schapira et al., 1990; Sherer et al., 2007).

Cytochrome P450 enzyme catalyzes the formation of epoxyeicosatrienoic acids (EETs) from arachidonic acid (AA). The EETs are converted to biologically inactive or less active diols by one of its major metabolising enzyme soluble epoxide hydrolase (sEH) (Spector, 2009). The cytoprotective role of EET's in various conditions are attributed to their ability to attenuate oxidative stress, inflammation, and apoptosis (Lakkappa et al., 2016; Spector and Norris, 2007). One of the novel strategies, therefore, is to inhibit the enzyme sEH and thereby promote the cytoprotective benefits of EETs in brain (Terashvili et al., 2012). EET's are broadly distributed in brain regions such as globus pallidus, substantia nigra, thalamus, cerebellum, pons, choroid plexus, medulla oblongata and hippocampus (Sura et al., 2008). The cytoprotective actions of EET's such as attenuation of oxidative stress, endoplasmic reticulum stress, inflammation, caspase activation and apoptosis in neuronal cells have been well studied and reported (Alkayed et al., 1996; Spector and Norris, 2007; Sura et al., 2008; Terashvili et al., 2012; Zhang et al., 2007). Our group has previously analyzed and reported the possible mechanisms of neuroprotective actions of EET's in PD (Lakkappa et al., 2016).

Therefore in the current study the administration of sEH inhibitors such as APAU will be tested. Since the inhibition of sEH, results in the elevation of EETs which are naturally occurring endogenous compounds, their elevation might not pose neurotoxicity or systemic toxicity. Which further eradicates the limitations of the current anti-parkinson therapies such as dopa-resistant motor (speech impairment, abnormal posture, gait and balance problems), nonmotor (autonomic dysfunction, mood and cognitive impairment, sleep problems, pain) complication and also drug-related side effects (especially psychosis, motor fluctuations, and dyskinesias) (Rascol et al., 2003a).

Earlier studies have reported a diverse class of sEH inhibitors such as amides, thioamides, ureas, thioureas, carbamates, acylhydrazones, chalcone oxides, and other pharmacophores to possess cytoprotective potential in various conditions (Morisseau and Hammock, 2013b; Shen, 2010). Among these the N, N'-disubstituted urea such as 12-(3-adamantan-1-yl-ureido)-dodecanoic acid (AUDA) and 1-adamantan-3-(5-(2-(2-ethylethoxy)ethoxy)pentyl)urea (AEPU) remained the most studied class of inhibitors because of their high potency. However, these inhibitors suffered from rapid *in vivo* metabolism (Anandan et al., 2009; Hwang et al., 2007; Kim et al., 2004; Liu et al., 2009; Morisseau et al., 1999, 2002; Tsai et al., 2010) and, therefore, the development was focused on piperidine- based di- and tri- substituted urea's, such as N-(1-(2,2,2-trifluoroethanoyl)piperidin-4-yl)-N'-(adamant-1-yl)urea (TPAU) and N-(1-acetylpiperidin-4-yl)-N-(adamant-1-yl)urea (APAU) (Jones et al., 2006). The structure activity relationship (SAR) studies on these molecules showed that the introduction of a conformationally restricted piperedine group resulted in improved metabolic stability (Liu et al., 2009; Rose et al., 2010). In the present study, sEH inhibitor APAU (Fig. 1) was evaluated against rotenone (ROT) induced neurodegeneration in N27 cell line and *Drosophila* model of PD to assess there neuroprotective benefits (Shen, 2010).

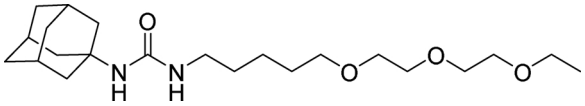

Fig. 1. Chemical structure of APAU.

2. Materials and methods

The sEH inhibitor, APAU was prepared by published procedures and the purity supported by proton and carbon NMR and LC- mass spectrometry as well as chromatographic support of purity (Hwang et al., 2013; Jones et al., 2006; Kim et al., 2007; Morisseau et al., 2002; Pecic et al., 2012; Rose et al., 2010) (Fig. 1). Rotenone, cell culture consumables, α-dinitrophenyl (DNP) antibody and protease inhibitor cocktail were purchased from Sigma (Sigma Aldrich, India). Fetal calf serum for cell culture was obtained from PAN Biotech (GmBh, Germany). Horseradish peroxidase (HRP) conjugated secondary antibodies were obtained from Bangalore Genei (Bangalore, Karnataka, India). Nitrocellulose membrane was obtained from Millipore (Billerica, MA, USA). Antibodies for JNK, phospho-JNK, c-jun, phospho-c-jun, and caspase-3 were obtained from Abcam (Abcam, MA, USA). The primers SOD, CAT, IL-6, EPHX-2, COX-1 and COX-2 were obtained from Eurofins Genomics. All other chemicals and reagents used were of analytical grade and purchased from SD fine Chemicals.

2.1. Docking studies

Docking studies were carried out using Glide, version 6.5, Schrödinger Suite 2012-14, LLC, New York, 2014-2, on a Maestro graphical user interface.

2.1.1. Ligand structure preparation

The structures of all the molecules were drawn using ChemBioDraw Ultra (Version 12, PerkinElmer Inc.). These structures were then subjected to ligand preparation process using LigPrep module of Glide. The energy minimization was carried out by using Optimized Potentials for Liquid Simulations-2005 (OPLS2005) force field.

2.1.2. Protein structure preparation

The X-ray crystal structure of the human sEH co-crystallized with ligand N-(2,4-dichlorobenzyl)-4-(pyrimidin-2-yloxy) piperidine-1-carboxamide (CIU) (PDB ID: 1VJ5) at 2.35 Å resolution was retrieved from the RCSB Protein Data Bank (PDB) and used to model the protein structures. In general, the protein structure was refined for their bond orders, formal charges and missing hydrogen atoms, topologies, incomplete and missing residues and terminal amide groups. The water molecules beyond 5 Å of the hetero atom were removed. The possible ionization states were generated for the heteroatom present in the protein structure and the most stable state was chosen. The hydrogen bonds were assigned and orientations of the retained water molecules

were corrected. Finally, a restrained minimization of the protein structure was carried out using OPLS 2005 force field to reorient side-chain hydroxyl groups and alleviate potential steric clashes.

2.1.3. Receptor grid generation

The prepared protein was used for the receptor grid construction. The various potential energies of the binding site of the protein were calculated based on the grid with a box size of 17 Å. In the receptor grid of the sEH- protein, the flexibility was assigned to the hydroxyl groups of tyrosine 334, 381, 465 and aspartate 333.

2.1.4. Validation of docking programme

The extra precision docking accuracy was validated by comparing the docked pose of ligand to the co-crystallized ligand pose. The Root Mean Square Deviation (RMSD) between the predicted conformation and the observed X-ray crystallographic conformation were used for the validation of the programme.

2.1.5. Glide ligand docking

The ligand docking was carried out using the previously prepared receptor grid and the ligand molecules. The favourable interactions between ligand molecules and the receptor were scored using the Glide ligand docking program (rigid docking mode). All the docking calculations were performed using the Extra Precision (XP) mode and the force field employed was OPLS 2005.

2.2. In vitro neurprotective activity

2.2.1. Sample preparation

The sample stock solutions were prepared by dissolving the 10 mg of APAU separately in 1 ml of DMSO. The further dilutions were made using serum free cell culture media. Rotenone toxin (10 mg) was freshly prepared by dissolving in 1 ml of DMSO and further dilutions were made using serum free cell culture media for the *in vitro* evaluation. All other reagent for antioxidant studies was freshly prepared before the experiments.

2.2.2. Cell culture and maintenance

The N27 ($1RB_3AN_{27}$) rat doapminergic cell lines have been used. The cell line was procured form Dr. Curt Freed, University of Colorado (U.S.A.). The cells were grown in nutrient RPMI medium 1640 containing 10% fetal bovine serum (FBS) and 1X antibiotic solution (100 U/ml penicillin, 100 µg/ml streptomycin and 0.25 g/ml amphotericin). Cell lines were maintained in a humid atmosphere of 5% CO_2 and 95% O_2 at 37 °C.

2.2.3. Neuroprotection studies

The sEH inhibitor APAU was screened for cytoxicity (at 24 h and 48 h) on N27 cell lines at a concentration range of 0.5–30 µM. The ROT induced cytoxicity was evaluated by treating the N27 cell lines with ROT (50–500 nM) for 24 h. Further the molecule was screened for its neuroprotective propensity (below its cytotoxic doses) against ROT (400 nM) induced toxicity. The cells were seeded into 96 well plates (for cell viability assays) and 6 well plates (for evaluation of oxidative stress, inflammatory, apoptotic parameters). After 24 h of cell seeding the cells was pre-treated with sEH inhibitor APAU for 3 h followed by ROT (400 nM) and incubated for 24 h. After 24 h the cell viability was assessed (using cells seeded in 96 well plates) by MTT and LDH release assay (Pandareesh and Anand, 2013; Vanderlinde, 1985; Wróblewski and Ladue, 1955). The cells in the 6 well plates were homogenized using cell lysis buffer (2% Triton X-100), and the homogenate was used for protein and other biochemical assays encompassing of ROS, hydroperoxides, lipid peroxidation, protein oxidation, mitochondrial complex-1, superoxide dismutase (SOD), catalase (CAT), glutathione peroxidise (GPx), glutathione reductase (GR), glutathione (GSH), and total antioxidant status (TAC) studies.

2.2.4. Redox assays (Detail procedure Table S3)

Redox assay	Procedure	Reference
ROS	After the treatment the intracellular ROS was estimated by the oxidation-sensitive dye 2′,7′- dichlorfluorescein-diacetate (DCFDA). The fluorescence intensity was measured at an excitation wavelength of 485 nm and an emission wavelength of 535 nm using Multi-technology plate reader (Tecan GmbH, Germany).	Jagatha et al. (2008), Ramadasan-Nair et al. (2014)
Hydroperoxide	Total cellular hydroperoxides were measured using commercially available Amplex red kit (A22188, Invitrogen) as per the manufacturer's instructions.	Gay et al. (1999)
Lipid peroxidation	The lipid peroxidation was estimated by using thiobarbituric acid (TBARS) with minor modifications, and the malondialdehyde (MDA) content was calculated using a molar extinction coefficient of $1.56 \times 10^5 M^{-1} cm^{-1}$	Garcia et al. (2005)
Mitochondrial membrane potential	The mitochondrial membrane potential (MMP) was estimated by using fluorescent dye rhodamine 123 (10 mg/ml) and the fluorescence intensity was measured at excitation wavelength of 485 nm and an emission wavelength of 535 nm using Multi-technology plate reader (Tecan GmbH, Germany).	Pandareesh et al. (2016a)
SOD	The activity of SOD was estimated by measuring degree of inhibition of quercetin oxidation. The quercetin at pH 10 undergoes oxidation due to free radical chain reaction involving superoxides and hence inhibitable by superoxide dismutase (SOD).	Kostyuk and Potapovich (1989)
CAT	CAT was estimated by measuring the decay of 6 mM H_2O_2 solution at 240 nm by the spectrophotometric degradation method. An extinction coefficient of 43.6 $M^{-1} cm^{-1}$ was used to determine the enzyme activity and values were expressed as mmol H_2O_2 degraded/min/mg of protein.	Aebi (1984)
GPx	Glutathione peroxidase (GPx) catalyzes the oxidation of glutathione (GSH) by cumene hydroperoxide. In the presence of glutathione reductase (GR) and NADPH the oxidized glutathione (GSSG) is immediately converted to reduced form with a concomitant oxidation of NADPH to $NADP^+$. The decrease in absorbance was measured at 340 nm.	Flohé and Günzler (1984)
GR	Glutathione reductase (GR) catalyses the reduction of oxidized glutathione (GSSG) to reduced glutathione (GSH) in presence of NADPH, which is oxidized to $NADP^+$. The decrease in absorbance was measured at 340 nm.	Saydam et al. (1997)
GSH	The total GSH was estimated by the 5, 5′ dithiobis 2-nitrobenzoic acid (DTNB) recycling method.	Banerjee et al. (1999), Mythri et al. (2007)
TAC	Total antioxidant capacity was determined by ABTS radicals scavenging assay. Decolourization of ABTS on a time-scale represents the antioxidant activity of sEH inhibitors. The concentration of the antioxidant and the duration of the reaction were monitored at 734 nm for 3 min at an interval of 1 min Multi-technology plate reader (Tecan GmbH, Germany).	Pandareesh et al. (2016a), Re et al. (1999)
Protein oxidation	The ROS induced oxidative modification of proteins was estimated by the method of oxyblot. The carbonyl groups in the protein side chains are derivatized to 2,4-dinitrophenylhydrazone	Butterfield and Stadtman (1997)

	(DNP-hydrazone) by reaction with 2,4-dinitrophenylhydrazine (DNPH) and estimated by the method of oxyblot

2.2.5. Mitochondrial complex I assay

The mitochondrion was isolated from N27 cells based on the principal of differential centrifugation. N27 cells were washed in buffer H (5 mM HEPES, 210 mM mannitol, 70 mM sucrose, 1 mM EGTA, and 0.5% bovine serum albumin) and were resuspended in the same buffer. The cell suspension was homogenized and centrifuged at 800 × *g* for 5 min at 4 °C. The supernatant that was enriched in mitochondria was then centrifuged at 10,000 × *g* for 20 min at 4 °C. The resulting mitochondrial pellet was resuspended in buffer H and stored as aliquots at −80 °C for estimation of proteins and complex I activity. The complex I assay was carried out according to standard protocol (Mythri et al., 2007; Pandareesh et al., 2016b). The specific activities with and without ROT were calculated independently. The difference between the two was taken as the activity specific to mitochondrial complex I (Mythri et al., 2007; Pandareesh et al., 2016b).

2.2.6. Estimation of Apoptotic markers by western blot analysis

JNK, phospho-JNK, c-jun, phospho-c-jun, caspase-3 and β-actin expression were analyzed by western blotting. Total cellular protein was separated on SDS-PAGE and transferred onto a nitrocellulose membrane using an electro blotting apparatus (Bio-Rad, Hercules, CA, USA). After the transfer the membrane was probed against primary antibody β-actin (ab8227), c-jun (ab32137), phospho-c-jun (ab32385), JNK (55 A8), phosho-JNK (98F2), pro and active caspase 3 (ab13585) (Abcam, MA, USA) all (1:500) dilution, followed by horseradish peroxidase conjugated secondary antibodies (goat anti-rabbit and anti-mouse antibodies) (Millipore, Billerica, MA, USA) (1:10,000) dilution. The membranes were washed and developed using a chemiluminescence, and the band intensities were captured using advanced gel doc systems (G: BOXChemi XT4, Syngene, MD, USA) and the band intensity was measured using NIH image J analysis software (Pandareesh et al., 2016b).

2.2.7. Total RNA isolation, c-DNA synthesis and quantitative PCR

The total RNA was isolated from N27 cells using RNeasy spin columns (Qiagen, USA) as per the manufacturer's instructions. The cDNA conversion was performed using commercial kit (Applied Biosystems (4368814) (CA, USA)). The transcript abundance of antioxidant genes such as SOD, CAT, inflammatory markers IL-6, COX-1 and COX-2, sEH gene EPHX-2 were examined by quantitative PCR. GAPDH was used as housekeeping gene. The primer design was performed using Integrated DNA technologies (IDT) and primer-BLAST software (Table S2). The PCR reaction mixture containing 2X Eva green PCR ready mix (containing dNTPs, 10 µl Taq-Polymerase), 2 ng of total cDNA, and 10 pmol forward and reverse primers (Eurofins, India) in a final volume of 20 µl. The cycling program was set as follows: one cycle of reverse transcription at 50 °C for 10 min, and 5 min of polymerase activation at 95 °C followed by 45 cycles of PCR at 95 °C for 10 s, 58 °C for 30 s. The threshold cycle (Ct) of the gene of interest, housekeeping gene and the difference between their Ct values (ΔCt) were determined. Normalized gene expression was calculated using Life-technologies 7500 software v2.0.6 (Pandareesh et al., 2016b).

2.3. In vivo neuroprotective activity

2.3.1. Sample preparation

The sample stock solutions were prepared by dissolving the 10 mg of APAU in 1 ml of DMSO. The further dilutions were made using sucrose solution (7% v/v) in sterile water. ROT toxin (500 µM) was freshly prepared by dissolving in DMSO and further dilutions were made using sucrose solution (7% v/v) in sterile water for the *in vivo* evaluation. All other reagent for antioxidant studies was freshly prepared before the experiments.

2.3.2. Drosophila husbandry and treatment

The wild type (Oregon K) adult, male, synchronized 10 day old flies were grown and maintained at 24 ± 1 °C, with 70–80% relative humidity and fed on a standard wheat flour-agar diet with yeast granules as the protein source (Hosamani, 2009, 2010). A pilot study was carried out by exposing the synchronized flies to ROT (10–1000 µM) and APAU (50–1000 µM) separately for about 12 days to determine the dose required to produce 50% death on days 8. Based on the results 500 µM ROT (LD_{50}: 500 µM), 50, 100 and 250 µM APAU (LD_{50} > 1000 µM) were selected for the neuroprotection studies (Fig. 7a and b). The flies were divided into 4 groups consisting of 50 flies in each group. Group 1 and 2 received vehicle DMSO (0.25% v/v) in sucrose solution (7% v/v)). Group 3 and 4 received APAU at a concentration of 50, 100 and 250µM, respectively. The vehicle and test solutions were administered as soaked filter paper discs. All treatments were started 4 days before ROT treatment. On day 6 all groups received ROT (500µM) except normal. The flies were subjected to negative geotaxis study daily and sacrificed on day 12 by freezing at -80 °C for 3 min. *Drosophila* heads were separated using a sharp cutter from the rest of body and stored at -80∘C for analysis of ROS, hydroperoxide, GSH, dopamine and its metabolites.

2.3.3. Negative geotaxis assay

Twenty adult male synchronized flies were transferred into a vertical glass column (Length, 25 cm; diameter, 1.5 cm) sealed on the other end. After a brief period of recovery, the flies were gently tapped to the bottom of the column. After a minute of recovery, the number of flies reaching the top of the column and the flies remained in the bottom of the column were counted separately. The data were expressed as percent flies crossed 10 cm mark in 60 s (Pandareesh et al., 2016b).

2.3.4. Redox assay in Drosophila

The heads of 20 flies from each group were separated and homogenized in sodium-phosphate buffer (0.1 M; pH 7.4) followed by centrifugation (2500 × *g* for 10 min at 4 °C). The supernatant was collected and used for estimation of ROS (Jagatha et al., 2008; Ramadasan-Nair et al., 2014), hydroperoxide (Gay et al., 1999) and GSH (Banerjee et al., 1999; Mythri et al., 2007) using protocol as employed in *in vitro* studies.

2.3.5. Estimation of Dopamine and its metabolites in Drosophila by LC–MS/MS

The pooled 40 flies' whole body homogenate was mixed with 1.25 *g* of activated charcoal and was agitated over night for removal of endogenous analytes. The extract was further filtered using Whatman filter paper. The filtrate was spiked with dopamine, DOPAC, HVA and L-phenylalanine (internal standard (IS)) at a concentration range of 5–2000 ng/ml. The proteins were precipitated with acetonitrile, centrifuged at 5000 × g rpm for 10 min. The 10 µl of clear supernatant of calibration standards and samples were injected into UFLC-ESI-QQQ mass spectrometer (Shimadzu 8030, Japan). The data acquisition was performed by using Lab solutions software (Shimadzu, Japan). The chromatographic separation was achieved on Jones C18 (50 × 4.6 mm; 3µ). The mobile phase was a mixture of methanol (A) and 0.1% acetic acid (B) in the ratio of 20:80 (v/v) with a flow rate of 0.5 ml/min isocratic elution mode. Detection was performed using positive (dopamine (154.05 > 137.05) and IS (166.15 > 120.10) and negative (DOPAC (167.05 > 123.10) and HVA (181.05 > 137.15)) MRM modes. DA, DOPAC and HVA were quantified by response factor (peak area of analyte/peak area of IS) and expressed in ng/mg protein (Phan et al., 2013) (Fig. S4 and Table 3).

2.4. Determination of protein

Protein concentrations in N27 cells and *Drosophila* head

homogenates were determined by the Bradford method using bovine serum albumin as standard (Bradford, 1976).

2.5. Statistical analysis

The data were expressed as the mean ± standard deviation (SD). Statistical significance was determined by one way ANOVA followed by Bonferroni *post hoc* test to assess differences between the groups. Values were considered significant, if $p < 0.05$.

3. Results

3.1. In silico docking study

The docking programme validation results reveal a very good agreement between the localization of ligand upon docking and the crystal structure. The RMSD between the predicted conformation and the observed X-ray crystallographic conformation of the ligand N-(2,4-dichlorobenzyl)-4-(pyrimidin-2-yloxy) piperidine-1-carboxamide was found to be 0.130 (Figure S2).

The results reveal a good glide score of APAU. The molecules received lipophilic, hydrophobic enclosure, hydrophobically Packed H-bond, hydrophobically packed correlated H-bond, hydrogen bonding, electrostatic, site map and low molecular weight rewards. In addition, the molecules received rotatable bond penalties (Table S1). The sEH inhibitor, APAU showed hydrogen bond with tyrosine 334, 381, 465 and aspartate 333 residues and these interactions were similar to co-crystal sEH inhibitor N-cyclohexyl-N'-(4-iodophenyl)urea (PDB ID: 1VJ5-CIU) (Figure S3). This confirms the good binding ability of the inhibitor.

3.2. In vitro neuroprotection study

The ROT at a dose of 400 nM produced significant cell death (approximately 50%) and induced significant changes in oxidative, inflammatory and apoptotic parameters when compared to Control, indicating a significant neurodegeneration. APAU showed a significant protection against ROT induced changes in the neuronal cell viability and LDH leakage at a concentration range of 2.5–10 μM (Fig. 2a–c). APAU (2.5 μM) also attenuated the ROT induced changes in oxidative stress (total intracellular ROS, hydroperoxides, protein oxidation, lipid peroxidation, SOD, CAT, GSH, GPx, GR, TAC, mitochondrial complex-1 activity, and mitochondrial membrane potential), inflammation (IL-6, COX-1 and COX-2), and apoptotic parameters (JNK, phospho-JNK, c-jun, phospho-c-jun, and active caspase-3) (Tables 1–2; Figs. 4–6).

3.3. In vivo neuroprotection study

ROT exposure at 500 μM for 6 days induced approximately 50% mortality (Fig. 7a) and significantly altered oxidative stress parameters (ROS, hydroperoxide, GSH) and DA, DOPAC and HVA levels in *Drosophila* head when compared to control ($p < 0.05$), indicating a significant neurodegeneration. The molecule APAU showed significant decrease in mortality when compared to ROT induced neurodegeneration (Fig. 7c). APAU also attenuated the ROT induced changes in oxidative stress parameters, locomotor dysfunctioning and improved ROT induced alteration DA, DOPAC and HVA levels ($p < 0.05$) (Fig. 7d and Table 3).

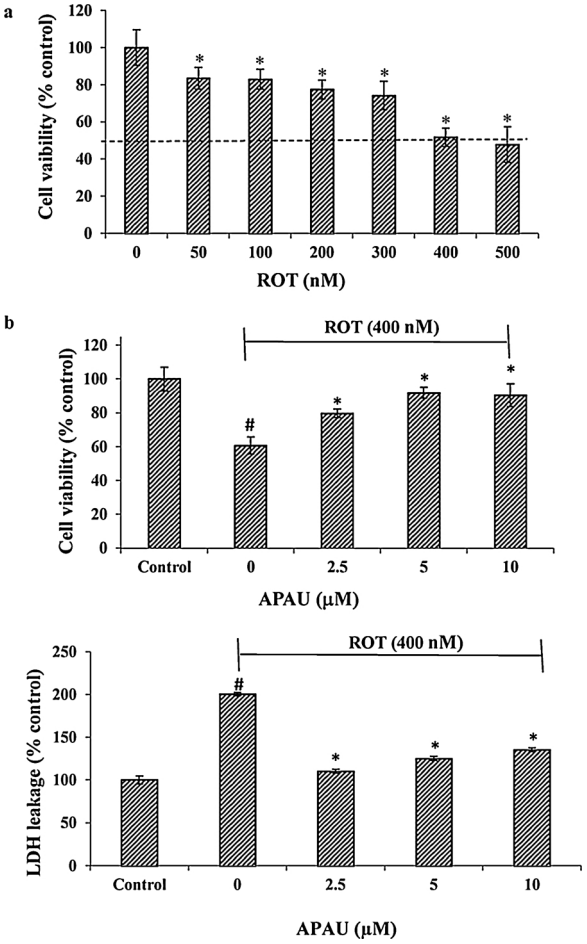

Fig. 2. (a) Dose dependent effect of ROT (1–500 nM) on N27 cell viability assessed by MTT assay. The data represent mean ± SEM of three independent experiments. $^{*}p < 0.05$ *versus* Control group. (b) Protective effect of APAU (2.5–10 μM/ml) against ROT (400 nM) induced cytotoxicity assessed by MTT assay. The data represent mean ± SEM of three independent experiments. $^{\#}p < 0.05$ *versus* Control group and $^{*}p < 0.05$ *versus* ROT group. (c) Protective effect of APAU (2.5–10 μM/ml) against ROT (400 nM) induced LDH leakage. The data represent mean ± SEM of three independent experiments. $^{\#}p < 0.05$ *versus* Control group and $^{*}p < 0.05$ *versus* ROT group.

4. Discussion

In the present study sEH inhibitor APAU was screened for its

Table 1
Effect of APAU on Oxidative stress parameters.

Grouping	ROS (% Control)	Hydroperoxide (% Control)	MDA levels (nmol/mg protein)	MMP (nmol/mg protein)
Control	100.0 ± 4.5	100.00 ± 1.3	16.13 ± 0.5	5.11 ± 0.24
ROT	294.8 ± 14.7$^{\#}$	141.70 ± 2.6$^{\#}$	28.29 ± 0.3$^{\#}$	2.65 ± 0.15$^{\#}$
APAU	97.9 ± 2.9	96.06 ± 1.2	15.43 ± 0.9	4.50 ± 0.25
ROT + APAU	226.8 ± 1.9$^{*\$}$	116.42 ± 1.9$^{*\$}$	15.55 ± 0.6*	4.25 ± 0.16*

Data express as mean ± SEM from three independent experiments. Different signs indicate statistically significant differences $^{\#}p < 0.05$ *versus* Control group; $^{*}p < 0.05$ *versus* ROT group and $^{\$}p < 0.05$ *versus* Control group.

Table 2
Effect of APAU on antioxidant enzyme activity.

Grouping	SOD (μg /mg protein)	CAT (mmol H_2O_2 degraded/mg protein)	Total GSH (μg/mg protein)	GR (μg/mg protein)	GPx (μg/mg protein)	TAC (μmol/mg protein)
Control	2.34 ± 0.05	0.85 ± 0.07	36.80 ± 2.75	4.12 ± 0.27	2.00 ± 0.03	3.41 ± 0.28
ROT	1.05 ± 0.02$^{\#}$	0.35 ± 0.07$^{\#}$	15.13 ± 2.08$^{\#}$	0.59 ± 0.04$^{\#}$	0.68 ± 0.03$^{\#}$	4.92 ± 0.25$^{\#}$
APAU	2.28 ± 0.05	0.65 ± 0.05	34.86 ± 2.83	3.48 ± 0.28	1.92 ± 0.035	3.22 ± 0.22
ROT + APAU	2.04 ± 0.06$^{*\$}$	0.62 ± 0.05$^{*\$}$	28.96 ± 2.08$^{*\$}$	2.33 ± 0.06$^{*\$}$	1.40 ± 0.14*	3.60 ± 0.33*

Data express as mean ± SEM from three independent experiments. Different signs indicate statistically significant differences $^{\#}p < 0.05$ *versus* Control group; $^{*}p < 0.05$ *versus* ROT group and $^{\$}p < 0.05$ *versus* Control group.

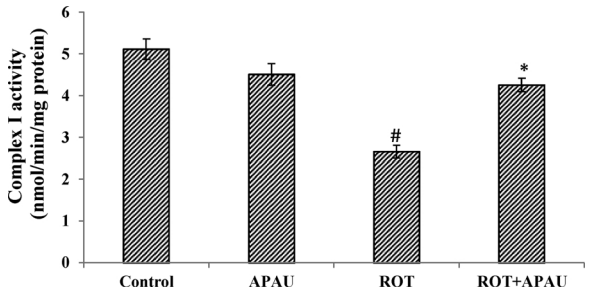

Fig. 3. Effect of APAU (2.5 μM/ml) on ROT (400 nM) induced altered mitochondrial complex I activity in N27 cell model. The data represent mean ± SEM of three independent experiments. $^{\#}p < 0.05$ *versus* control group and $^{*}p < 0.05$ *versus* rotenone group.

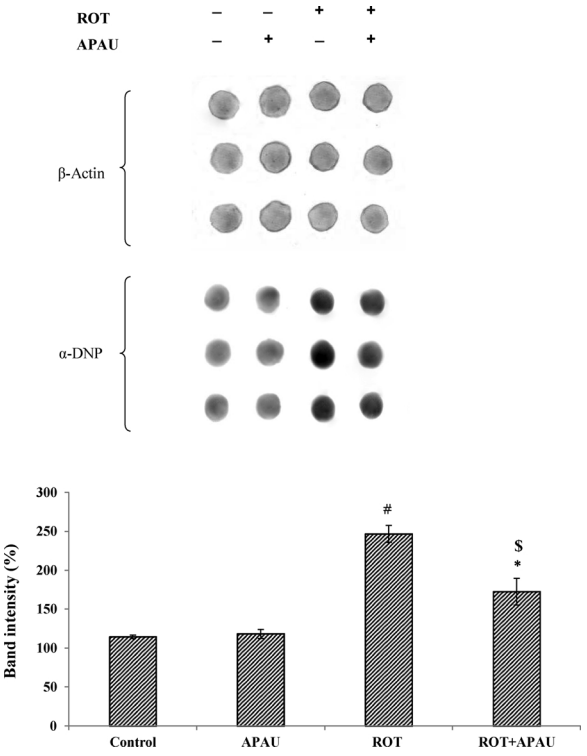

Fig. 4. Effect of APAU (2.5 μM/ml) on ROT (400 nM) induced protein oxidation, as determined by estimation of protein carbonyls by oxyblot. The data represent mean ± SEM of three independent experiments. $^{\#}p < 0.05$ *versus* Control group; $^{*}p < 0.05$ *versus* ROT group and $^{\$}p < 0.05$ *versus* Control group.

neuroprotection activity. *In silico* results confirm a good binding interaction of the molecules at the active site of sEH (PDB: 1VJ5) (Table S1 and Figure S3). ROT is a potent mitochondrial complex-I inhibitor reported to induce neurotoxicity specific to dopaminergic neurons through mitochondrial dysfunctioning, and ROS production (Alam and Schmidt, 2002; Panov et al., 2005). ROT induced disturbance in the natural oxidation and reduction equilibrium has been reported to induce oxidative stress mediated modifications to DNA, lipids, and proteins followed by activation of microglia and generation of pro-inflammatory mediators leading to apoptosis (Dexter et al., 1989; Floor and Wetzel, 1998; Liang et al., 2015) (Fig. 8).

The ROT induced inhibition of mitochondrial complex-1 leads to leakage of electron from respiratory chain resulting in generation of ROS. The increased ROS levels were significantly attenuated by pre-treatment with APAU as confirmed by DCFDA and hydroperoxide assay (Table 1). The sEH inhibitor APAU also significantly restored ROT mediated mitochondrial complex-I dysfunctioning (Guo et al., 2013) (Fig. 3). The abnormal increase in ROS levels results in peroxidation of membrane lipids and damage to mitochondrial membrane permeability. The pre-treatment with sEH inhibitors, APAU significantly attenuated the ROS induced lipid peroxidation and altered mitochondrial membrane potential as confirmed by TBARS and rhodamine 123 florescence assays (Table 1). Further the ROS mediated protein oxidation leads to loss of protein functions was significantly attenuated by APAU as confirmed in results of DNPH oxyblots (Fig. 4). In addition, the ROT induced decline in activity of anti-oxidant enzymes such as GSH, SOD, CAT, GR, and Gpx was significantly prevented by pre-treatment with APAU (Table 2). The beneficial effect of these molecules on the total anti-oxidant status was supported by the results of ABTS assay (Table 2).

A variety of studies over the last few years support the hypothesis that the broad activity of sEH inhibitors and the epoxy fatty acids is that they stabilize on many disease states, arise from a reduction in the endoplasmic reticulum stress response which is in turn stimulated by excess release of ROS (Sirish et al., 2016).

ROT is reported to decrease the mRNA expression of SOD, CAT which was significantly improved by pre-treatment with APAU (Fig. 6) (Javed et al., 2016). The ROT is also reported to stimulate activation microglia resulting in increased production of Pro-inflammatory mediators (Jiang et al., 2017; Klintworth et al., 2009; Tetsuka et al., 1996) such as IL-6, COX-1 and 2 which was significantly normalized by pre-treatment with APAU. These data support the anti-inflammatory role of APAU (Fig. 6). The ROT induced impaired cellular redox state results in stress induced activation of JNK1/2, c-jun phosphorylation, and caspase 3 resulting in apoptosis (Li et al., 2003; Moungjaroen et al., 2006). The current study results show that pre-treatment with APAU inhibited caspase 3 activation by preventing phosphorylation of JNK and c-jun. These molecule, therefore may act by inhibiting both intrinsic and extrinsic pathways of apoptosis (Dhanasekaran and Reddy, 2008; Liu

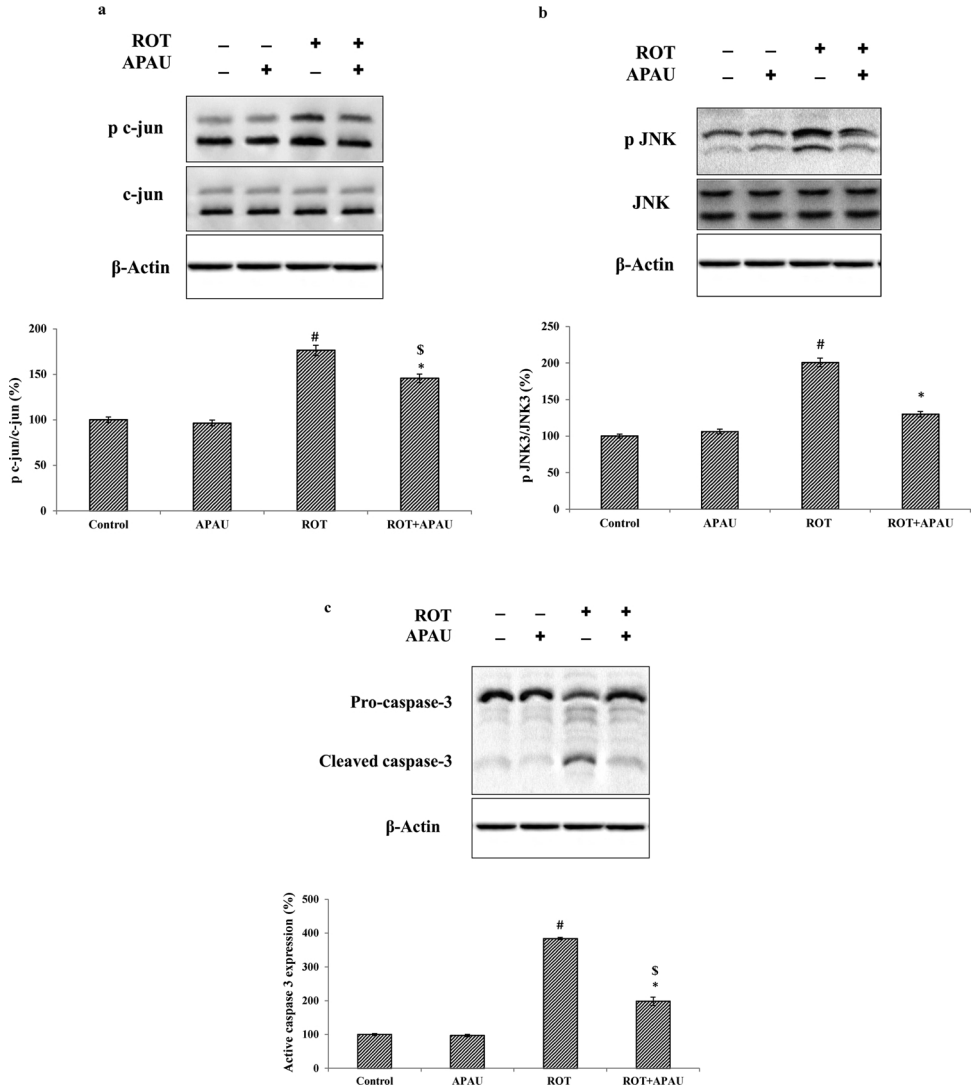

Fig. 5. (a–c): Effect of APAU (2.5 μM/ml) on ROT (400 nM) induced alterations in apoptotic marker proteins - phospho c-jun, phospho JNK and caspase 3 analyzed by using western blot. Quantification of the individual bands in the blot is represented by bar graphs below the blots. The data represent mean ± SEM of three independent experiments. $^{\#}p < 0.05$ *versus* control group; $^{*}p < 0.05$ *versus* ROT group and $^{\$}p < 0.05$ *versus* Control group.

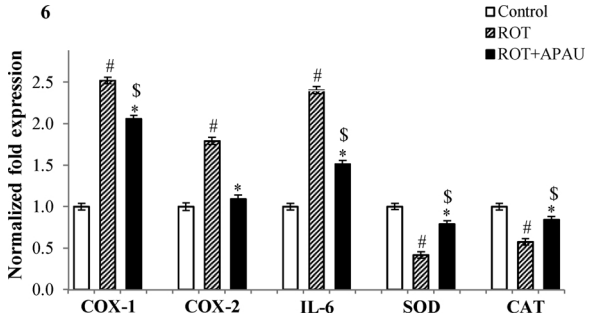

Fig. 6. Effect of APAU (2.5 μM/ml) on ROT (400 nM) induced altered expression of redox genes (SOD, CAT), and inflammatory markers (COX-1 and 2, IL-6) assessed by RT-PCR. The data represent mean ± SEM of three independent experiments. $^{\#}p < 0.05$ *versus* Control group; $^{*}p < 0.05$ *versus* ROT group and $^{\$}p < 0.05$ *versus* Control group.

et al., 2011; Ma et al., 2012) (Fig. 5a–c). Similar kind of studies were reported by Maia Terashvili and group, showing the neuroprotective role of 14,15-EET and sEH inhibitor, 12-(3-adamantan-1-yl-ureido)-dodecanoic acid (AUDA) against H_2O_2 induced neurodegeneration in N27 cell lines (Terashvili et al., 2012).

In the *Drosophila* model ROT treatment induced dose dependent mortality, locomotor dysfunctioning and dopamine depletion (Fig. 7a-d). Previously ROT was reported to induce site specific dopaminergic neurodegeneration *via* inhibition of mitochondrial complex-1 mediated ROS production in flies (Coulom and Birman, 2004). The pre-treatment with APAU significantly attenuated the ROT induced deficits including restoration of DA and its metabolites and antioxidant status (Table 3). The present study results therefore support the neuroprotective benefits of APAU. However, the use of APAU has advantages over current antiparkinson's medication, as they have no drug induced side effects. The elevation of endogenous EETs might not impose motor and non-motor dysfunctioning as seen in current antiparkinson's medications (Rascol et al., 2003a). Due to lack toxic effects of EET's, APAU might be a safe drug of choice, to be used as a prophylactic, in prevention of neurological disorders. Our study also reported the restoration of rotenone induced Complex-1 dysfunctioning which is one of the major cause of the neurodegeneration in PD (Schapira et al., 1990). In addition, studies have reported the elevated levels of EET's improve mitochondrial

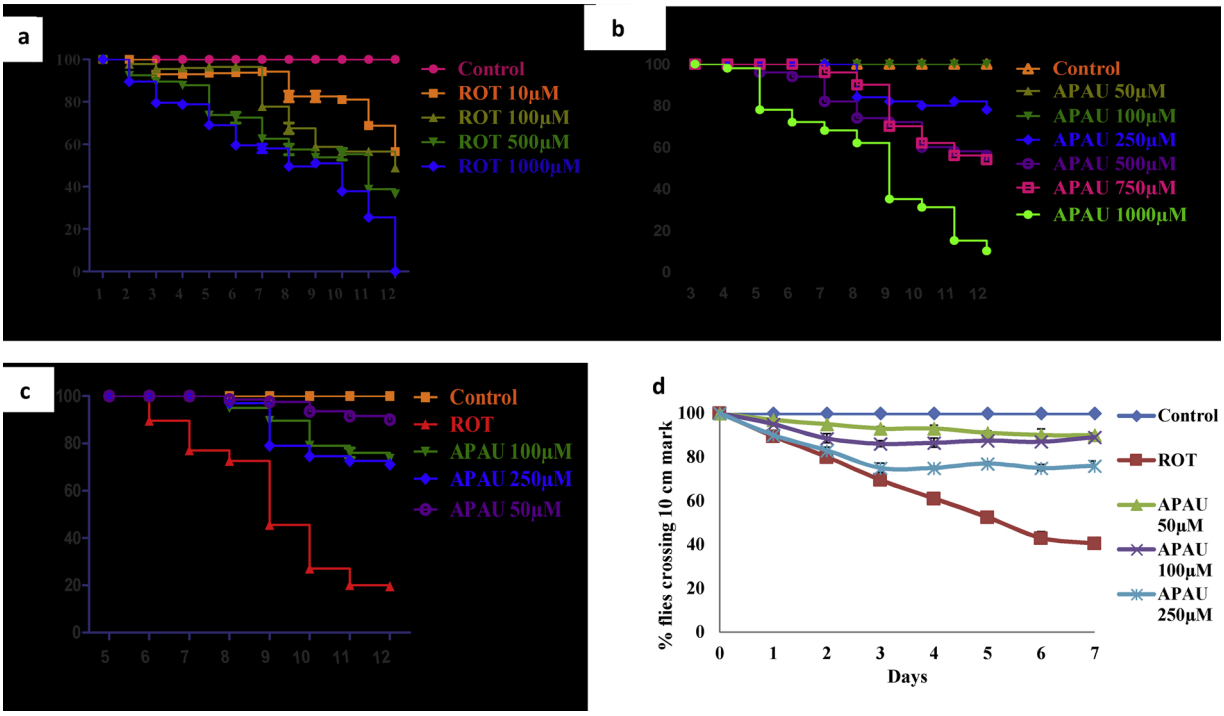

Fig. 7. a, b, c, and d: Protective effect of APAU on ROT-induced mortality and locomotor deficits in the *Drosophila* model of PD. Dose dependent lethality response expressed as percent mortality among adult male *Drosophila* exposed to various concentration of ROT (10–1000 µM) and APAU (50–1000 µM) is shown in Fig. 7a, and b; c shows the % mortality among the flies pre-treated with APAU (50–100 µM) for 5 days, followed by co-treated with both APAU and ROT for 7 days. Fig. 7d shows the improvement in the locomotor deficits by APAU (50–100 µM) as determined by negative geotaxis assay. The data represented in percentage, where n = 2. Analyzed by using one way analysis of variance followed by Bonferroni post test.

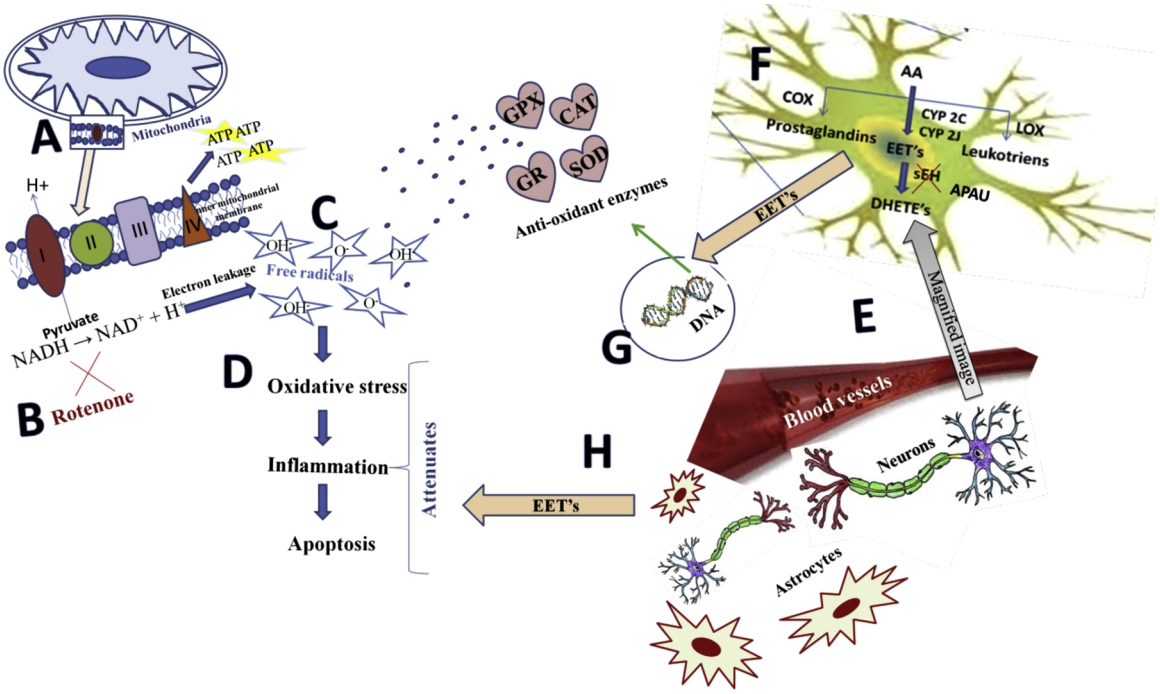

Fig. 8. sEH inhibitors APAU mediated neuroprotection against ROT induced toxicity.

functions in cardiac cells (Akhnokh et al., 2016; Batchu et al., 2012). However, the exact mechanism of action of EET's on mitochondrial functions is still under research, which may indeed need further exploration. Since PD is a multiple neurodegenerative disorder, the reported simultaneous inhibition of oxidative stress, inflammation and apoptosis by EET's will have an added advantage over the current antiparkinson medication. Therefore, the use of APAU alone or in combination with existing drug therapy with dopamine replacement may prove to be a drug of choice for PD.

Table 3
Effect of APAU on ROS, Hydroperoxide, GSH, Dopamine and its metabolite against ROT induced toxicity in *Drosophila*.

	ROS levels (% Control)		Hydroperoxide levels (% Control)		GSH Levels (ng/mg protein)		DA and its metabolites (ng/mg protein)					
							Dopamine		DOPAC		DOPAC/DA	
	Head	Body	Head	Body	Head	Body	Head	Body	Head	Body	Head	Body
Control	100 ± 7.5	100 ± 3.03	100 ± 0.4	105.6 ± 0.7	16.76 ± 1.7	9.0 ± 0.8	1.33 ± 0.04	18863.8 ± 707.1	95.5 ± 1.3	71.63 ± 2.1	71.8 ± 0.6	263.3 ± 12
ROT	157.2 ± 7.1$^{\#}$	139.5 ± 6.1$^{\#}$	131.2 ± 14$^{\#}$	145.5 ± 13.9$^{\#}$	9.65 ± 0.3$^{\#}$	4.65 ± 0.1$^{\#}$	0.15 ± 0.01$^{\#}$	3504.0 ± 146.4$^{\#}$	62.1 ± 2.7$^{\#}$	23.62 ± 0.7$^{\#}$	396.3 ± 1.3$^{\#}$	148.3 ± 11$^{\#}$
APAU (50 μM)	86.1 ± 5.1$^{*\$}$	80.3 ± 3.8$^{*\$}$	77.3 ± 3.2$^{*\$}$	86.5 ± 1.4$^{*\$}$	15.5 ± 0.1*	8.1 ± 0.1*	0.7 ± 0.01$^{*\$}$	8007.1 ± 88.9$^{*\$}$	77.3 ± 2.4$^{*\$}$	38.30 ± 0.3$^{*\$}$	100.3 ± 0.2$^{*\$}$	155.2 ± 11$^{*\$}$
APAU (100 μM)	99.1 ± 1.8*	86.5 ± 6.8$^{*\$}$	80.15 ± 6.2$^{*\$}$	90.7 ± 13.4$^{*\$}$	15.4 ± 0.3*	7.93 ± 0.1$^{*\$}$	0.8 ± 0.01$^{*\$}$	8078.2 ± 98.9$^{*\$}$	87.3 ± 1.4*	48.30 ± 0.7$^{*\$}$	108.3 ± 0.7$^{*\$}$	167.2 ± 14$^{*\$}$
APAU (250 μM)	111.3 ± 4.1*	97.62 ± 0.9*	80.15 ± 6.2$^{*\$}$	75.3 ± 10.1$^{*\$}$	13.7 ± 0.1$^{*\$}$	7.3 ± 0.1$^{*\$}$	0.7 ± 0.01$^{*\$}$	13,077.0 ± 108.1$^{*\$}$	43.7 ± 0.7$^{*\$}$	50.22 ± 1.4$^{*\$}$	61.9 ± 0.3*	260.3 ± 20*

Data express as mean ± SEM from three independent experiments. Different signs indicate statistically significant differences $^{\#}p < 0.05$ *versus* Control group; $^{*}p < 0.05$ *versus* ROT group and $^{\$}p < 0.05$ *versus* Control group.

5. Conclusion

The study results concludes the sEH inhibitors, APAU, shows significant neuroprotective benefits. This molecule has the potential to target multiple neurodegenerative pathways and, therefore, can prevent disease progression. APAU, therefore, has a unique potential which is not available with the currently used antiparkison agents.

Transparency document

The Transparency document associated with this article can be found in the online version.

Funding

This work was partially supported by National Institute of Environmental Health Sciences (NIEHS), United States, (Grant number: ES002710). Bruce D. Hammock is a George and Judy Marcus senior fellow of the American Asthma Foundation.

Conflict of interest

The author declares that there is no conflict of interest.

Acknowledgements

We thank Dr. D. Velmurugan and Mr. D. Anantha Krishnan, Department of Crystallography and Biophysics, University of Madras, Guindy Campus, Chennai, India, for helping to carryout *in silico* studies.

Appendix A. Supplementary data

Supplementary data associated with this article can be found, in the online version, at https://doi.org/10.1016/j.neuro.2018.11.010.

References

Aebi, H., 1984. [13] Catalase in vitro. Meth. Enzymol. 105, 121–126.
Akhnokh, M.K., Yang, F.H., Samokhvalov, V., Jamieson, K.L., Cho, W.J., Wagg, C., Takawale, A., Wang, X., Lopaschuk, G.D., Hammock, B.D., 2016. Inhibition of soluble epoxide hydrolase limits mitochondrial damage and preserves function following ischemic injury. Front. Pharmacol. 7, 133.
Alam, M., Schmidt, W., 2002. Rotenone destroys dopaminergic neurons and induces parkinsonian symptoms in rats. Behav. Brain Res. 136 (1), 317–324.
Alkayed, N.J., Narayanan, J., Gebremedhin, D., Medhora, M., Roman, R.J., Harder, D.R., 1996. Molecular characterization of an arachidonic acid epoxygenase in rat brain astrocytes. Stroke 27 (5), 971–979.
Anandan, S.-K., Webb, H.K., Do, Z.N., Gless, R.D., 2009. Unsymmetrical non-adamantyl N, N′-diaryl urea and amide inhibitors of soluble expoxide hydrolase. Bioorg. Med. Chem. Lett. 19 (15), 4259–4263.
Banerjee, B., Seth, V., Bhattacharya, A., Pasha, S., Chakraborty, A., 1999. Biochemical effects of some pesticides on lipid peroxidation and free-radical scavengers. Toxicol. Lett. 107 (1), 33–47.
Batchu, S.N., Lee, S.B., Samokhvalov, V., Chaudhary, K.R., El-Sikhry, H., Weldon, S.M., Seubert, J.M., 2012. Novel soluble epoxide hydrolase inhibitor protects mitochondrial function following stress. Can. J. Physiol. Pharmacol. 90 (6), 811–823.
Bonnet, A., Houeto, J., 1999. Pathophysiology of Parkinson's disease. Biomed. Pharmacother. 53 (3), 117–121.
Bradford, M.M., 1976. A rapid and sensitive method for the quantitation of microgram quantities of protein utilizing the principle of protein-dye binding. Anal. Biochem. 72 (1-2), 248–254.
Butterfield, D.A., Stadtman, E.R., 1997. Protein oxidation processes in aging brain. Adv. Cell Aging Gerontol. 2, 161–191.
Caraceni, T., Geminiani, G., Tamma, F., 1989. Current approaches in the treatment of Parkinson disease. Recenti Prog. Med. 80 (12), 686–691.
Coulom, H., Birman, S., 2004. Chronic exposure to rotenone models sporadic Parkinson's disease in Drosophila melanogaster. J. Neurosci. 24 (48), 10993–10998.
Cummings, J.L., 1992. Depression and Parkinson's disease: a review. Am. J. Psychiatry 149 (4), 443.
De Virgilio, A., Greco, A., Fabbrini, G., Inghilleri, M., Rizzo, M.I., Gallo, A., Conte, M., Rosato, C., Appiani, M.C., de Vincentiis, M., 2016. Parkinson's disease: Autoimmunity and neuroinflammation. Autoimmun. Rev. 15 (10), 1005–1011.
DeLong, M., Wichmann, T., 2009. Pathophysiology of Parkinson's Disease, Textbook of Stereotactic and Functional Neurosurgery. Springer, pp. 1497–1506.

Dexter, D., Carter, C., Wells, F., Javoy-Agid, F., Agid, Y., Lees, A., Jenner, P., Marsden, C.D., 1989. Basal lipid peroxidation in substantia nigra is increased in Parkinson's disease. J. Neurochem. 52 (2), 381–389.
Dhanasekaran, D.N., Reddy, E.P., 2008. JNK signaling in apoptosis. Oncogene 27 (48), 6245–6251.
Esposito, E., Cuzzocrea, S., 2010. New therapeutic strategy for Parkinson's and Alzheimer's disease. Curr. Med. Chem. 17 (25), 2764–2774.
Flohé, L., Günzler, W.A., 1984. [12] Assays of glutathione peroxidase. Meth. Enzymol. 105, 114–120.
Floor, E., Wetzel, M.G., 1998. Increased protein oxidation in human substantia nigra pars compacta in comparison with basal ganglia and prefrontal cortex measured with an improved dinitrophenylhydrazine assay. J. Neurochem. 70 (1), 268–275.
Garcia, Y.J., Rodríguez-Malaver, A.J., Peñaloza, N., 2005. Lipid peroxidation measurement by thiobarbituric acid assay in rat cerebellar slices. J. Neurosci. Methods 144 (1), 127–135.
Gay, C., Collins, J., Gebicki, J.M., 1999. Hydroperoxide assay with the ferric–xylenol orange complex. Anal. Biochem. 273 (2), 149–155.
Guo, C., Sun, L., Chen, X., Zhang, D., 2013. Oxidative stress, mitochondrial damage and neurodegenerative diseases. Neural Regen. Res. 8 (21), 2003.
Hosamani, R., 2009. Neuroprotective efficacy of Bacopa monnieri against rotenone induced oxidative stress and neurotoxicity in Drosophila melanogaster. Neurotoxicology 30 (6), 977–985.
Hosamani, R., 2010. Prophylactic Treatment With Bacopa monnieri Leaf Powder Mitigates Paraquat-induced Oxidative Perturbations and Lethality in Drosophila melanogaster.
Hwang, S.H., Tsai, H.-J., Liu, J.-Y., Morisseau, C., Hammock, B.D., 2007. Orally bioavailable potent soluble epoxide hydrolase inhibitors. J. Med. Chem. 50 (16), 3825.
Hwang, S.H., Wecksler, A.T., Zhang, G., Morisseau, C., Nguyen, L.V., Fu, S.H., Hammock, B.D., 2013. Synthesis and biological evaluation of sorafenib-and regorafenib-like sEH inhibitors. Bioorg. Med. Chem. Lett. 23 (13), 3732–3737.
Jagatha, B., Mythri, R.B., Vali, S., Bharath, M.S., 2008. Curcumin treatment alleviates the effects of glutathione depletion in vitro and in vivo: therapeutic implications for Parkinson's disease explained via in silico studies. Free Radic. Biol. Med. 44 (5), 907–917.
Jankovic, J., Aguilar, L.G., 2008. Current approaches to the treatment of Parkinson's disease. Neuropsychiatr. Dis. Treat. 4 (4), 743–757.
Javed, H., Azimullah, S., Khair, S.B.A., Ojha, S., Haque, M.E., 2016. Neuroprotective effect of nerolidol against neuroinflammation and oxidative stress induced by rotenone. BMC Neurosci. 17 (1), 58.
Jiang, X., Feng, X., Huang, H., Liu, L., Qiao, L., Zhang, B., Yu, W., 2017. The effects of rotenone-induced toxicity via the NF-κB-iNOS Pathway in rat liver. Toxicol. Mech. Methods 1–22 (just-accepted).
Jones, P.D., Tsai, H.-J., Do, Z.N., Morisseau, C., Hammock, B.D., 2006. Synthesis and SAR of conformationally restricted inhibitors of soluble epoxide hydrolase. Bioorg. Med. Chem. Lett. 16 (19), 5212–5216.
Kim, I.-H., Morisseau, C., Watanabe, T., Hammock, B.D., 2004. Design, synthesis, and biological activity of 1, 3-disubstituted ureas as potent inhibitors of the soluble epoxide hydrolase of increased water solubility. J. Med. Chem. 47 (8), 2110–2122.
Kim, I.-H., Tsai, H.-J., Nishi, K., Kasagami, T., Morisseau, C., Hammock, B.D., 2007. 1, 3-Disubstituted ureas functionalized with ether groups are potent inhibitors of the soluble epoxide hydrolase with improved pharmacokinetic properties. J. Med. Chem. 50 (21), 5217–5226.
Klintworth, H., Garden, G., Xia, Z., 2009. Rotenone and paraquat do not directly activate microglia or induce inflammatory cytokine release. Neurosci. Lett. 462 (1), 1–5.
Kostyuk, V.A., Potapovich, A.I., 1989. Superoxide-driven oxidation of quercetin and a simple sensitive assay for determination of superoxide dismutase. Biochem. Int. 19 (5), 1117–1124.
Lakkappa, N., Krishnamurthy, P.T., Hammock, B.D., Velmurugan, D., Bharath, M.S., 2016. Possible role of Epoxyeicosatrienoic acid in prevention of oxidative stress mediated neuroinflammation in Parkinson disorders. Med. Hypotheses 93, 161–165.
Li, N., Ragheb, K., Lawler, G., Sturgis, J., Rajwa, B., Melendez, J.A., Robinson, J.P., 2003. Mitochondrial complex I inhibitor rotenone induces apoptosis through enhancing mitochondrial reactive oxygen species production. J. Biol. Chem. 278 (10), 8516–8525.
Liang, Y., Jing, X., Zeng, Z., Bi, W., Chen, Y., Wu, X., Yang, L., Liu, J., Xiao, S., Liu, S., 2015. Rifampicin attenuates rotenone-induced inflammation via suppressing NLRP3 inflammasome activation in microglia. Brain Res. 1622, 43–50.
Liu, J.Y., Tsai, H.J., Hwang, S.H., Jones, P.D., Morisseau, C., Hammock, B.D., 2009. Pharmacokinetic optimization of four soluble epoxide hydrolase inhibitors for use in a murine model of inflammation. Br. J. Pharmacol. 156 (2), 284–296.
Liu, L., Chen, C., Gong, W., Li, Y., Edin, M.L., Zeldin, D.C., Wang, D.W., 2011. Epoxyeicosatrienoic acids attenuate reactive oxygen species level, mitochondrial dysfunction, caspase activation, and apoptosis in carcinoma cells treated with arsenic trioxide. J. Pharmacol. Exp. Ther. 339 (2), 451–463.
Ma, J., Zhang, L., Han, W., Shen, T., Ma, C., Liu, Y., Nie, X., Liu, M., Ran, Y., Zhu, D., 2012. Activation of JNK/c-Jun is required for the proliferation, survival, and angiogenesis induced by EET in pulmonary artery endothelial cells. J. Lipid Res. 53 (6), 1093–1105.
Morisseau, C., Hammock, B.D., 2013a. Impact of soluble epoxide hydrolase and epoxyeicosanoids on human health. Annu. Rev. Pharmacol. Toxicol. 53, 37–58.
Morisseau, C., Hammock, B.D., 2013b. Impact of soluble epoxide hydrolase and epoxyeicosanoids on human health. Annu. Rev. Pharmacol. Toxicol. 53, 37.
Morisseau, C., Goodrow, M.H., Dowdy, D., Zheng, J., Greene, J.F., Sanborn, J.R., Hammock, B.D., 1999. Potent urea and carbamate inhibitors of soluble epoxide hydrolases. Proc. Natl. Acad. Sci. 96 (16), 8849–8854.
Morisseau, C., Goodrow, M.H., Newman, J.W., Wheelock, C.E., Dowdy, D.L., Hammock, B.D., 2002. Structural refinement of inhibitors of urea-based soluble epoxide hydrolases. Biochem. Pharmacol. 63 (9), 1599–1608.
Moungjaroen, J., Nimmannit, U., Callery, P.S., Wang, L., Azad, N., Lipipun, V., Chanvorachote, P., Rojanasakul, Y., 2006. Reactive oxygen species mediate caspase activation and apoptosis induced by lipoic acid in human lung epithelial cancer cells through Bcl-2 down-regulation. J. Pharmacol. Exp. Ther. 319 (3), 1062–1069.
Mullin, S., Schapira, A.H., 2015. Pathogenic mechanisms of neurodegeneration in Parkinson disease. Neurol. Clin. 33 (1), 1–17.
Mythri, R.B., Jagatha, B., Pradhan, N., Andersen, J., Bharath, M.S., 2007. Mitochondrial complex I inhibition in Parkinson's disease: how can curcumin protect mitochondria? Antioxid. Redox Signal. 9 (3), 399–408.
Oertel, W., Schulz, J.B., 2016. Current and experimental treatments of Parkinson disease: A guide for neuroscientists. J. Neurochem. 139, 325–337.
Pandareesh, M., Anand, T., 2013. Neuromodulatory propensity of Bacopa monniera against scopolamine-induced cytotoxicity in PC12 cells via down-regulation of AChE and up-regulation of BDNF and muscarnic-1 receptor expression. Cell. Mol. Neurobiol. 33 (7), 875–884.
Pandareesh, M., Anand, T., Bhat, P.V., 2016a. Cytoprotective propensity of Bacopa monniera against hydrogen peroxide induced oxidative damage in neuronal and lung epithelial cells. Cytotechnology 68 (1), 157–172.
Pandareesh, M., Shrivash, M., Kumar, H.N., Misra, K., Bharath, M.S., 2016b. Curcumin monoglucoside shows improved bioavailability and mitigates rotenone induced neurotoxicity in cell and drosophila models of Parkinson's disease. Neurochem. Res. 1–16.
Panov, A., Dikalov, S., Shalbuyeva, N., Taylor, G., Sherer, T., Greenamyre, J.T., 2005. Rotenone model of parkinson disease multiple brain mitochondria dysfunctions after short term systemic rotenone intoxication. J. Biol. Chem. 280 (51), 42026–42035.
Pecic, S., Deng, S.-X., Morisseau, C., Hammock, B.D., Landry, D.W., 2012. Design, synthesis and evaluation of non-urea inhibitors of soluble epoxide hydrolase. Bioorg. Med. Chem. Lett. 22 (1), 601–605.
Perfeito, R., Cunha-Oliveira, T., Rego, A.C., 2012. Revisiting oxidative stress and mitochondrial dysfunction in the pathogenesis of Parkinson disease—resemblance to the effect of amphetamine drugs of abuse. Free Radic. Biol. Med. 53 (9), 1791–1806.
Phan, N.T., Hanrieder, Jr., Berglund, E.C., Ewing, A.G., 2013. Capillary electrophoresis–Mass spectrometry-based detection of drugs and neurotransmitters in Drosophila brain. Anal. Chem. 85 (17), 8448–8454.
Quinn, N., 1995. Drug treatment of Parkinson's disease. BMJ Br. Med. J. 310 (6979), 575.
Ramadasan-Nair, R., Gayathri, N., Mishra, S., Sunitha, B., Mythri, R.B., Nalini, A., Subbannayya, Y., Harsha, H.C., Kolthur-Seetharam, U., Bharath, M.M.S., 2014. Mitochondrial alterations and oxidative stress in an acute transient mouse model of muscle degeneration implications for muscular dystrophy and related muscle pathologies. J. Biol. Chem. 289 (1), 485–509.
Rascol, O., Payoux, P., Ory, F., Ferreira, J.J., Brefel-Courbon, C., Montastruc, J.L., 2003a. Limitations of current Parkinson's disease therapy. Ann. Neurol. 53 (S3), S3–S15.
Rascol, O., Payoux, P., Ory, F., Ferreira, J.J., Brefel-Courbon, C., Montastruc, J.L., 2003b. Limitations of current Parkinson's disease therapy. Ann. Neurol. 53 (S3), S3–S15.
Re, R., Pellegrini, N., Proteggente, A., Pannala, A., Yang, M., Rice-Evans, C., 1999. Antioxidant activity applying an improved ABTS radical cation decolorization assay. Free Radic. Biol. Med. 26 (9), 1231–1237.
Rose, T.E., Morisseau, C., Liu, J.-Y., Inceoglu, B., Jones, P.D., Sanborn, J.R., Hammock, B.D., 2010. 1-Aryl-3-(1-acylpiperidin-4-yl) urea inhibitors of human and murine soluble epoxide hydrolase: structure – activity relationships, pharmacokinetics, and reduction of inflammatory pain. J. Med. Chem. 53 (19), 7067–7075.
Saydam, N., Kirb, A., Demir, Ö., Hazan, E., Oto, Ö., Saydam, O., Güner, G., 1997. Determination of glutathione, glutathione reductase, glutathione peroxidase and glutathione S-transferase levels in human lung cancer tissues. Cancer Lett. 119 (1), 13–19.
Schapira, A., 2005. Present and future drug treatment for Parkinson's disease. J. Neurol. Neurosurg. Psychiatr. 76 (11), 1472–1478.
Schapira, A., Cooper, J., Dexter, D., Clark, J., Jenner, P., Marsden, C., 1990. Mitochondrial complex I deficiency in Parkinson's disease. J. Neurochem. 54 (3), 823–827.
Shen, H.C., 2010. Soluble epoxide hydrolase inhibitors: a patent review. Expert Opin. Ther. Pat. 20 (7), 941–956.
Sherer, T.B., Richardson, J.R., Testa, C.M., Seo, B.B., Panov, A.V., Yagi, T., Matsuno-Yagi, A., Miller, G.W., Greenamyre, J.T., 2007. Mechanism of toxicity of pesticides acting at complex I: relevance to environmental etiologies of Parkinson's disease. J. Neurochem. 100 (6), 1469–1479.
Sirish, P., Li, N., Timofeyev, V., Zhang, X.-D., Wang, L., Yang, J., Lee, K.S.S., Bettaieb, A., Ma, S.M., Lee, J.H., 2016. Molecular mechanisms and new treatment paradigm for atrial fibrillation. Circ. Arrhythm. Electrophysiol. 9 (5), e003721.
Spector, A.A., 2009. Arachidonic acid cytochrome P450 epoxygenase pathway. J. Lipid Res. 50 (Supplement), S52–S56.
Spector, A.A., Norris, A.W., 2007. Action of epoxyeicosatrienoic acids on cellular function. Am. J. Physiol.-Cell Physiol. 292 (3), C996–C1012.
Spillantini, M.G., Schmidt, M.L., Lee, V.M.-Y., Trojanowski, J.Q., Jakes, R., Goedert, M., 1997. α-Synuclein in Lewy bodies. Nature 388 (6645), 839–840.
Stefanis, L., 2012. α-Synuclein in Parkinson's disease. Cold Spring Harb. Perspect. Med. 2 (2), a009399.
Sura, P., Sura, R., EnayetAllah, A.E., Grant, D.F., 2008. Distribution and expression of

soluble epoxide hydrolase in human brain. J. Histochem. Cytochem. 56 (6), 551–559.
Terashvili, M., Sarkar, P., Van Nostrand, M., Falck, J.R., Harder, D.R., 2012. The protective effect of astrocyte-derived 14, 15-EET on H2O2-induced cell injury in astrocyte-dopaminergic neuronal cell line co-culture. Neuroscience 223, 68.
Tetsuka, T., Baier, L.D., Morrison, A.R., 1996. Antioxidants inhibit interleukin-1-induced cyclooxygenase and nitric-oxide synthase expression in rat mesangial cells evidence for post-transcriptional regulation. J. Biol. Chem. 271 (20), 11689–11693.
Tsai, H.-J., Hwang, S.H., Morisseau, C., Yang, J., Jones, P.D., Kasagami, T., Kim, I.-H., Hammock, B.D., 2010. Pharmacokinetic screening of soluble epoxide hydrolase inhibitors in dogs. Eur. J. Pharm. Sci. 40 (3), 222–238.
Vanderlinde, R.E., 1985. Measurement of total lactate dehydrogenase activity. Ann. Clin. Lab. Sci. 15 (1), 13–31.
Wróblewski, F., Ladue, J.S., 1955. Lactic Dehydrogenase Activity in Blood. Proc. Soc. Exp. Biol. Med. 90 (1), 210–213.
Zhang, W., Koerner, I.P., Noppens, R., Grafe, M., Tsai, H.-J., Morisseau, C., Luria, A., Hammock, B.D., Falck, J.R., Alkayed, N.J., 2007. Soluble epoxide hydrolase: a novel therapeutic target in stroke. J. Cereb. Blood Flow Metab. 27 (12), 1931–1940.